Nat Med. Author manuscript; available in PMC 2017 October 18.

Published in final edited form as:
Nat Med. 2015 February ; 21(2): 166–172. doi:10.1038/nm.3766.

Inhibiting peripheral serotonin synthesis reduces obesity and metabolic dysfunction by promoting brown adipose tissue thermogenesis

Justin D Crane[1,2,7], **Rengasamy Palanivel**[1,3,4,7], **Emilio P Mottillo**[1], **Adam L Bujak**[1], **Huaqing Wang**[3,4], **Rebecca J Ford**[1], **Andrew Collins**[1], **Regje M Blümer**[1], **Morgan D Fullerton**[1], **Julian M Yabut**[1], **Janice J Kim**[3,4], **Jean-Eric Ghia**[3], **Shereen M Hamza**[5], **Katherine M Morrison**[2], **Jonathan D Schertzer**[2,6], **Jason R B Dyck**[5], **Waliul I Khan**[3,4], and **Gregory R Steinberg**[1,6]

[1]Division of Endocrinology and Metabolism, Department of Medicine, McMaster University, Hamilton, Ontario, Canada

[2]Department of Pediatrics, McMaster University, Hamilton, Ontario, Canada

[3]Farncombe Family Digestive Health Research Institute, McMaster University, Hamilton, Ontario, Canada

[4]Department of Pathology and Molecular Medicine, McMaster University, Hamilton, Ontario, Canada

[5]Cardiovascular Research Centre, Alberta Diabetes Institute, Department of Pediatrics, Faculty of Medicine and Dentistry, University of Alberta, Edmonton, Alberta, Canada

[6]Department of Biochemistry and Biomedical Sciences, McMaster University, Hamilton, Ontario, Canada

Abstract

Mitochondrial uncoupling protein 1 (UCP1) is enriched within interscapular brown adipose tissue (iBAT) and beige (also known as brite) adipose tissue[1,2], but its thermogenic potential is reduced with obesity and type 2 diabetes[3–5] for reasons that are not understood. Serotonin (5-hydroxytryptamine, 5-HT) is a highly conserved biogenic amine that resides in non-neuronal and neuronal tissues that are specifically regulated via tryptophan hydroxylase 1 (Tph1) and Tph2, respectively[6–8]. Recent findings suggest that increased peripheral serotonin[9] and polymorphisms in *TPH1* are associated with obesity[10]; however, whether this is directly related to reduced BAT

Correspondence should be addressed to W.I.K. (khanwal@mcmaster.ca) or G.R.S. (gsteinberg@mcmaster.ca).
[7]These authors contributed equally to this work.

AUTHOR CONTRIBUTIONS

J.D.C., R.P., E.P.M., K.M.M., J.R.B.D., W.I.K. and G.R.S. designed the experiments. J.D.C., R.P., E.P.M., H.W., S.M.H. and A.L.B. performed the *in vivo* animal experiments and testing. E.P.M., J.M.Y. and R.M.B. performed the cell experiments. J.D.C., R.P., E.P.M., A.L.B., J.M.Y. R.J.F., M.D.F., J.D.S., H.W., J.J.K., J.-E.G. and A.C. provided technical expertise and performed data analyses. J.D.C. W.I.K. and G.R.S. wrote the manuscript. All authors edited the manuscript and provided comments.

COMPETING FINANCIAL INTERESTS

The authors declare no competing financial interests.

Note: Any Supplementary Information and Source Data files are available in the online version of the paper.

thermogenesis and obesity is not known. We find that *Tph1*-deficient mice fed a high-fat diet (HFD) are protected from obesity, insulin resistance and nonalcoholic fatty liver disease (NAFLD) while exhibiting greater energy expenditure by BAT. Small-molecule chemical inhibition of Tph1 in HFD-fed mice mimics the benefits ascribed to *Tph1* genetic deletion, effects that depend on UCP1-mediated thermogenesis. The inhibitory effects of serotonin on energy expenditure are cell autonomous, as serotonin blunts β-adrenergic induction of the thermogenic program in brown and beige adipocytes *in vitro*. As obesity increases peripheral serotonin, the inhibition of serotonin signaling or its synthesis in adipose tissue may be an effective treatment for obesity and its comorbidities.

Serotonin is a primal signaling molecule conserved across phyla that is implicated in the control of energy balance[11]. Central serotonin is known to regulate energy balance by decreasing appetite through effects on the nervous system. The majority of serotonin in the body is produced by the enzyme Tph1 (ref. 6). $Tph1^{-/-}$ mice exhibit very low levels of circulating serotonin, but maintain normal levels of serotonin in the brain due to the inability of serotonin to cross the blood-brain barrier and the sustained presence of Tph2 which controls central serotonin production[8]. In contrast $Tph2^{-/-}$ mice have low central serotonin, impaired growth and autonomic function, and exhibit poor maternal care and disrupted sleep patterns[12]. While $Tph1^{-/-}$ mice have no behavioral differences, studies have indicated an important role for this enzyme in suppressing lipolysis and hepatic glucose production[13], inhibiting inflammation[14] and enhancing insulin secretion during pregnancy[15]. While we found minor differences in body mass and adiposity of $Tph1^{-/-}$ mice fed a chow diet, in agreement with previous reports[15], these mice had normal glucose and insulin tolerance compared to wild-type ($Tph1^{+/+}$) controls (Supplementary Fig. 1a–d). However, when fed a HFD, $Tph1^{-/-}$ mice gained significantly less weight (Fig. 1a) and had lower adiposity (Fig. 1b) and expression of markers of adipose tissue inflammation (Fig. 1c) than wild-type mice. HFD-fed $Tph1^{-/-}$ mice also had lower liver weights characterized by less lipid accumulation than wild-type mice (Fig. 1d), indicating protection from NAFLD. Obesity also contributes to the development of insulin resistance and dysglycemia. Consistent with less adiposity, $Tph1^{-/-}$ mice had lower fed blood glucose (Fig. 1e) and fasting serum insulin (Fig. 1f) and improved glucose tolerance (Fig. 1g) and insulin sensitivity (Fig. 1h,i) compared to HFD-fed wild-type mice. These data indicate that $Tph1^{-/-}$ mice are protected from obesity and related metabolic diseases, including NAFLD and insulin resistance.

To examine the mechanisms contributing to the attenuated weight gain of HFD-fed $Tph1^{-/-}$ mice, we examined energy intake and expenditure using metabolic cages. There was no difference in mean daily food intake between HFD-fed groups ($Tph1^{+/+}$: 2.4 ± 0.2 g and $Tph1^{-/-}$: 2.4 ± 0.2 g, $P = 0.65$, $n = 12$ per group, data are mean ± s.e.m.), and previous studies have found that deletion of Tph1 does not influence gut motility or nutrient absorption[16]. Physical activity levels were also comparable between HFD-fed mice ($Tph1^{+/+}$: 205 ± 20 and $Tph1^{-/-}$: 228 ± 20 mean beam breaks per 20 min, $P = 0.41$, $n = 12$ per group, data are mean ± s.e.m); however, oxygen consumption was greater in $Tph1^{-/-}$ mice during both dark and light cycles and during periods of inactivity than in wild-type mice (Fig. 1j), thus indicating a greater basal metabolic rate.

To determine which tissues contributed to the increase in basal metabolic rate, we measured [^{18}F]fluorodeoxyglucose (FDG) uptake using positron emission tomography–computed tomography (PET-CT) and found that FDG uptake was higher in the iBAT of HFD-fed *Tph1*$^{-/-}$ mice compared to wild-type mice, but there was no difference in muscle, liver or heart (Fig. 2a). Given the predominant changes in iBAT metabolic activity of *Tph1*$^{-/-}$ mice, we measured serotonin content in this tissue and found that it was elevated with a HFD in wild-type but not *Tph1*$^{-/-}$ mice (Fig. 2b). Consistent with the increased metabolic activity and reductions in serotonin content, iBAT from HFD-fed *Tph1*$^{-/-}$ mice had higher UCP1 content than that from wild-type mice (Fig. 2c). In addition, anesthetized HFD-fed *Tph1*$^{-/-}$ mice had higher basal oxygen uptake (Fig. 2d) and inter-scapular surface temperatures than HFD-fed wild-type mice (Fig. 2e), differences that were maintained following treatment with the β_3-adrenergic agonist CL-316,243. These findings indicate that the anti-obesity effect of genetic *Tph1* deletion is associated with greater BAT thermogenesis.

To examine whether the loss of serotonin was mediating the metabolic effects in HFD-fed *Tph1*$^{-/-}$ mice, we implanted slow-release (60-d) serotonin or placebo pellets. Serotonin pellets induced a modest increase in circulating serotonin versus placebo when implanted into *Tph1*$^{-/-}$ mice pellets (Supplementary Fig. 2a), although the level achieved in HFD-fed *Tph1*$^{-/-}$ mice was still lower than what is achieved by diet-induced obesity in wild-type mice[9]. Although there was no detectable difference in body mass (Supplementary Fig. 2b), potentially owing to the relatively small increase in serotonin levels, HFD-fed *Tph1*$^{-/-}$ mice implanted with serotonin pellets had an ~20% greater epididymal white adipose tissue (eWAT) weight compared to those implanted with the placebo (Supplementary Fig. 2c). Additionally, the greater peripheral serotonin levels induced by serotonin pellets compared to placebo in *Tph1*$^{-/-}$ mice was associated with higher fed blood glucose and lowered glucose tolerance and insulin sensitivity (Supplementary Fig. 2d–f). HFD-fed *Tph1*$^{-/-}$ mice implanted with the serotonin pellet also had a lower basal metabolic rate than *Tph1*$^{-/-}$ mice implanted with the placebo, despite no differences in cage activity or food intake (Supplementary Fig. 2g–i). In addition, when challenged with CL-316,243, HFD-fed *Tph1*$^{-/-}$ mice implanted with serotonin pellets had an attenuated stimulation of oxygen uptake and a tendency for lower thermogenesis compared to *Tph1*$^{-/-}$ mice implanted with placebo pellets (Supplementary Fig. 2j, absolute value data demonstrate the same effect). These findings indicate that Tph1-mediated regulation of serotonin directly regulates BAT activity *in vivo*.

To examine the mechanism by which serotonin may regulate BAT activity, we examined concentrations of catecholamines (epinephrine, norephinephrine and dopamine) in the urine as a readout of sympathetic tone and found that, unexpectedly, they were lower in HFD-fed *Tph1*$^{-/-}$ mice compared to wild-type mice, whereas adipose tissue catecholamine levels were unchanged (Supplementary Table 1). These data suggested that serotonin may be altering the sensitivity of BAT to β-adrenergic stimulation. As β-adrenergic signaling is transmitted via cyclic AMP (cAMP), we assessed basal iBAT cAMP levels and found they were higher in HFD-fed *Tph1*$^{-/-}$ mice compared to the levels in HFD- wild-type mice (Fig. 2f). HFD-fed *Tph1*$^{-/-}$ mice also had greater basal and CL-316,243–stimulated phosphorylation of protein kinase A (PKA) substrates in BAT tissue than HFD-fed wild-type

mice (Fig. 2g). These data indicate that the iBAT of *Tph1*$^{-/-}$ mice has enhanced sensitivity to β-adrenergic stimulation.

To determine whether serotonin could alter cAMP levels and the induction of the thermogenic program in a cell-autonomous manner, we treated iBAT cells originally derived from C57BL/6 mice[17] with serotonin before stimulation with isoproterenol (a β-adrenergic agonist). Serotonin attenuated isoproterenol-stimulated cAMP accumulation (Fig. 2h) and phosphorylation of the PKA substrate hormone- sensitive lipase (HSL, Fig. 2i). This effect was not seen with serotonin precursors (tryptophan, 5-hydroxytryptophan (5-HTP)) or end products (5HIAA, melatonin, Supplementary Fig. 3a). Notably, serotonin treatment blunted the induction of *Ucp1* expression after isoproterenol treatment in the iBAT cells (Fig. 2j). Thus, serotonin acts directly on brown adipocytes to suppress β-adrenergic induction of *Ucp1*.

Recent studies have established that inhibition of gut-derived Tph1 with the small molecule LP533401 effectively treats irritable bowel syndrome[18] and osteoporosis[19] without affecting brain serotonin content. LP533401 has low oral bioavailability[18]; therefore, to ensure effective delivery of the compound to BAT, we performed intraperitoneal injections into HFD-fed C57BL/6 mice for 12 weeks. We found that injection of LP533401 resulted in lower circulating serotonin levels in mice compared to vehicle in HFD-fed mice (Fig. 3a). As anticipated, HFD-fed mice treated with vehicle (5% DMSO in water) gained ~1–2 g per week over the treatment period, but this weight gain was lower in mice treated with LP533401 (Fig. 3b). Similar to the effects of genetic *Tph1* deletion, LP533401 treatment resulted in a lower accumulation of body fat (Fig. 3c and Supplementary Table 2), reductions in liver mass and lipid levels (Fig. 3d), improvements in glucose homeostasis (Fig. 3e,f) and greater insulin sensitivity (Fig. 3g) versus vehicle. Notably, we obtained comparable results when the mice were first made obese by HFD feeding for 8 weeks before the initiation of daily Tph1 inhibitor treatment (Supplementary Fig. 4a–f). Therefore, chemical inhibition of Tph1 phenocopies the effects of *Tph1* genetic deletion, preventing and reversing obesity, NAFLD and insulin resistance.

To examine the mechanisms contributing to the prevention of weight gain in LP533401-treated mice, we placed HFD-fed mice in metabolic cages after 12 d of treatment, which was before any apparent change in body mass (vehicle: 29.4 ± 0.6 versus LP533401: 28.9 ± 0.6 g, $n = 8$ per group, data are mean ± s.e.m.). LP533401 treatment resulted in higher oxygen consumption during both the dark and light cycles compared to vehicle (Fig. 3h) with no differences in cage activity (vehicle: 340 ± 51 versus LP533401: 392 ± 31 mean beam breaks per 20 min, $P = 0.65$, $n = 8$ per group, data are mean ± s.e.m.) or daily food intake (vehicle: 2.2 ± 0.1 versus LP533401: 2.3 ± 0.1 g, $P = 0.96$, $n = 8$ per group, data are mean ± s.e.m.). The changes in energy expenditure were also unrelated to alterations in heart rate or blood pressure, which were comparable between vehicle- and LP533401-treated mice (Supplementary Fig. 5a–c). Additionally, angiogenic gene expression in iBAT was not different between wild-type and *Tph1*$^{-/-}$ mice, suggesting that blood supply was not influenced by inhibition of Tph1 (Supplementary Fig. 5d); however, we cannot discount the possible influence of Tph1 inhibition on changes within the local microvasculature. We subsequently performed FDG PET-CT analysis and found that mice treated with LP533401

had greater FDG uptake in iBAT than vehicle-treated mice (Fig. 3i), which is consistent with higher expression of UCP1 and lower lipid deposition in iBAT (Fig. 3j). These data demonstrate that chemical Tph1 inhibition increases energy expenditure and BAT activity.

As beige adipocytes can also contribute to adipose tissue thermogenesis[20,21], we examined FDG uptake into abdominal fat from HFD-fed *Tph1*$^{+/+}$ and *Tph1*$^{-/-}$ mice and HFD-fed C57BL/6 mice treated with vehicle or LP533401. We found that both genetic (Supplementary Fig. 6a) and chemical (Supplementary Fig. 6b) ablation of *Tph1* resulted in greater FDG uptake into abdominal fat compared to wild-type and vehicle-treated mice, respectively (owing to the resolution of the CT, it is not possible to determine which specific fat depot this was occurring in). The higher abdominal fat FDG uptake in *Tph1*$^{-/-}$ and LP533401-treated mice was accompanied by a gene signature consistent with the 'browning' of WAT (Supplementary Fig. 6c–e). Serotonin treatment also blunted the induction of *Ucp1* in beige adipocytes derived from the stromal vascular fraction of inguinal WAT (Supplementary Fig. 6f), indicating that serotonin inhibits the browning of WAT via a direct mechanism analogous to observations in iBAT.

The enhanced metabolic capacity of brown and beige adipose tissue is dependent on the expression of UCP1. Therefore, to establish whether the metabolic benefits of Tph1 inhibition (reductions in body mass, NAFLD and glycemia) are derived from increased UCP1-mediated thermogenesis, we performed daily injections of LP533401 in UCP1-null (*Ucp1*$^{-/-}$) and wild-type (*Ucp1*$^{+/+}$) littermates fed a HFD and housed under thermoneutral conditions (30 °C). Whereas UCP1 activity and expression are suppressed under thermoneutral conditions compared to that observed in mice raised at lower temperatures, UCP1 nevertheless counteracts obesity, as evidenced by the greater weight gain in HFD-fed *Ucp1*$^{-/-}$ mice housed at thermoneutrality[22]. Remarkably, when treated with LP533401, *Ucp1*$^{+/+}$ mice, but not *Ucp1*$^{-/-}$ mice, had attenuated weight gain (Fig. 4a) and lower adiposity (Fig. 4b) (time course of body weights is in Supplementary Fig. 7a,b). The suppressive effects of LP533401 on eWAT inflammation (Supplementary Fig. 7c) and serum interleukin-6 abundance (Supplementary Fig. 7d) compared to vehicle occurred in both genotypes, indicating that the anti-inflammatory effects of Tph1 inhibition are independent of weight loss. In contrast, wild-type mice treated with LP533401 had lower liver weights (Fig. 4c) and lipid content (Fig. 4d), as well as greater glucose tolerance (Fig. 4e), than wild-type mice treated with vehicle and both groups of *Ucp1*$^{-/-}$ mice. Furthermore, when challenged with CL-316,243, only *Ucp1*$^{+/+}$ mice treated with LP533401exhibited an increase in oxygen uptake and thermogenesis (Fig. 4f,g). Thus, the metabolic benefits of Tph1 inhibition require UCP1-mediated thermogenesis.

Serotonin was discovered more than 60 years ago and was aptly named for its presence in serum (sero) and its vasoactive properties (tonin)[23]. Central serotonergic pathways are involved in the effects of several appetite-suppressing drugs (including fenfluramine and sibutarmine) and in enhancing sympathetic outflows to BAT[24]. Elevations in peripheral serotonin caused by a HFD[9] have not been widely investigated, although obesity has been associated with lower circulating tryptophan levels[25] and serotonin synthesis is increased in mice on a Western diet[26], suggesting that enhanced Tph1 activity accompanies obesity. Additionally, peripheral serotonin has been shown to inhibit thyroid function in rats[27],

although its role in altering energy expenditure or thermogenesis was not known. To this end, we inhibited *Tph1* using both genetic and pharmacological means, models that do not affect central serotonin, and found that HFD-induced obesity caused an elevation in BAT serotonin levels that is dependent on *Tph1*. Preventing obesity-induced increases in serotonin enhanced BAT activity and whole-body energy expenditure, protecting mice against obesity and related disorders including low-grade inflammation, insulin resistance and NAFLD. Whereas previous studies in *Caenorhabditis elegans* demonstrated that serotonin increases energy expenditure by upregulating fatty acid oxidation[28], our findings, showing the opposite in rodents, match contrasting observations between subphyla in relation to serotonin and appetite control[11]. The opposing effects of central compared to peripheral serotonin on BAT activity are also consistent with observations in other biological systems including bone[29] and the cardiovascular system[30].

Daily intraperitoneal injections of LP533401 in HFD-fed mice showed that chemical inhibition of Tph1 phenocopied the effects observed in *Tph1*$^{-/-}$ mice fed a HFD (increased energy expenditure, brown adipose tissue metabolism, weight loss and insulin sensitivity). This effect was also observed in mice housed under thermoneutral conditions but was absent in mice lacking UCP1, indicating the specificity of the response. A recent report in HFD-fed mice delivered a four fold higher dose of LP533401 (100 mg per kg body weight) via oral gavage showed no effect on body mass despite comparable reductions in plasma serotonin[13]. We believe the major difference between this previous report and our own is related to the mode of drug delivery. Because LP533401 has low oral bioavailability, very little of the compound reaches the circulation[18] compared to what would be achieved through intraperitoneal injections. These data suggest that Tph1 inhibition promotes energy expenditure and the thermogenic program by acting on cells other than the gastrointestinal tract.

Although weight loss has been observed in rats following chronic administration of very high doses of serotonin that result in lethargy and diarrhea (20–50 mg per kg body weight[31,32]), this level of dosing is more than 100-fold higher than that used in our serotonin pellet experiments, which were more closely aligned with the physiological increases observed with obesity[9]. We used only male mice in the current study, but Tph1 expression and central serotonin levels are influenced by gender and the estrous cycle[33], suggesting that peripheral serotonin synthesis may also be regulated in part by sex steroid hormones. Thus, it is possible that serotonin levels may be important in the differential regulation of BAT activity between men and women[3].

White adipocytes express a majority of the approximately 14 serotonin receptor types[32,34], and gene array studies in BAT cells have also identified the expression of the majority of these receptors[17,35]. Given that serotonin blunted β-adrenergic–induced increases in cAMP, the inhibitory effects of serotonin on BAT thermogenesis may be mediated via the 5HTR1, 5HTR4, 5HTR5, 5HTR6 or 5HTR7 receptor types, which have all been linked to changes in cAMP[36]. Thus, the regulation of serotonin and its mechanism of action on thermogenic adipocytes are not yet well understood. Moreover, although it is unlikely that tryptophan, 5-HTP or other serotonin pathway metabolites have direct effects on adipocytes, we cannot rule out their effects on other tissues, particularly because some of these compounds, unlike

serotonin, can cross the blood-brain barrier. Discordant levels of 5-HTP and serotonin have been described in *Tph1*$^{-/-}$ mice, in which 5-HTP levels are higher in the forebrain compared to wild-type littermates[37]. These data, in combination with the finding that tryptophan, serotonin or 5-HTP can increase metabolic rate when injected directly into the central nervous system[38], suggest the possibility that other serotonin-related metabolites may also regulate BAT thermogenesis.

In conclusion, we find that genetic or chemical inhibition of Tph1 protects or reverses the development of HFD-induced obesity and dysglycemia via activation of UCP1-mediated thermogenesis. Although several metabolites may induce adaptive thermogenesis in adipose tissue and attenuate obesity, such as retinaldehyde[39], β-aminoisobutyric acid[40] or locally released catecholamines[1], to our knowledge, serotonin is the first metabolite shown to be elevated in obesity that inhibits the activity of BAT or beige adipose tissue in mammals. Thus, inhibiting Tph1-derived serotonin may be effective in reversing obesity and related clinical disorders such as NAFLD and type 2 diabetes.

ONLINE METHODS

Animal housing and breeding

All experiments were approved by the McMaster University Animal Ethics Committee and conducted under the Canadian guidelines for animal research. Only male mice were used in experiments, and they were housed in specific pathogen–free microisolator cages that were located in a room maintained at a constant temperature of 23 °C (except for the *Ucp1*$^{-/-}$ colony) on a 12-h light-dark cycle with lights on at 7:00 a.m. All treatment groups were weight matched and randomized to treatment at the initiation of an experiment. The researcher conducting the experiments was not blinded to the experimental groups during testing. Animals were excluded from analysis if there were signs of fighting causing skin lesions or excessive wounds. *Tph1*$^{-/-}$ mice on a C57BL/6 background were originally acquired from F. Côté (CNRS/Université UMR, Paris, France)[41]. Heterozygous (*Tph1*$^{+/-}$) mice were interbred to generate *Tph1*$^{-/-}$ and *Tph1*$^{+/+}$ littermates. Starting at 8 weeks of age, male *Tph1*$^{-/-}$ and *Tph1*$^{+/+}$ mice received either a chow diet (17% kcal fat; Diet 8640, Harlan Teklad, Madison, WI) or high-fat diet (HFD, 45% kcal fat, D12451, Research Diets; New Brunswick, NJ) and water *ad libitum* for 12 weeks. For the initial chemical inhibitor studies, male C57BL/6 mice were purchased from The Jackson Laboratory at 6 weeks of age and immediately placed on the HFD described above. Starting at 8 weeks of age, HFD-fed C57BL/6 mice received a daily intraperitoneal injection of the Tph1 inhibitor LP533401 (25 mg kg^{-1} body weight, Dalton Pharma Services, Canada) dissolved in DMSO and diluted with water (5% DMSO final concentration) or equal volume of vehicle (5% DMSO in water). For the serotonin pellet studies in *Tph1*$^{-/-}$ mice, a single 60-d slow-release serotonin pellet (0.5 mg pellet^{-1}) or placebo pellet (Innovative Research of America) was implanted into the subcutaneous interscapular white fat in 10-week-old mice, and the skin cut was secured using surgical glue. Mice were monitored for a total of 8 weeks and were subjected to physiologic testing before killing. *Ucp1*-heterozygous mice were acquired from The Jackson Laboratory and bred to produce UCP1-null (*Ucp1*$^{-/-}$) and wild-type (*Ucp1*$^{+/+}$) littermates. In order to prevent thermal stress, mice in this colony were bred and housed in a

room maintained at 30 °C. Mice were then placed on a HFD and treated with the Tph1 inhibitor as described above. All testing except for the CL–316,243 challenge occurred at this temperature. All data are presented as mean ± s.e.m.

Metabolic and blood measurements

Metabolic monitoring was performed in a Comprehensive Lab Animal Monitoring System (CLAMS, Columbus Instruments, OH, USA) as described[42]. To specifically assess UCP1-mediated thermogenesis, CL-316,243 challenge experiments were performed using the CLAMS equipment and surface interscapular thermogenesis as described[43]. All metabolic monitoring occurred in a room kept between 26 and 28 °C. Insulin and glucose tolerance tests were performed after 16 weeks of the diet intervention in *Tph1*$^{-/-}$ mice experiments and after 6–10 weeks of HFD in LP533401 injection experiments as previously described[44]. For serum insulin measurements, fasting and fed blood samples were collected by retro-orbital bleed between weeks 16 and 18 using a non-heparinized capillary tube as described[45]. For circulating serotonin analyses, blood was collected from the mandibular (Fig. 3a) or tail (Supplementary Fig. 2a) vein using heparinized capillary tubes. Blood samples were then transferred to Eppendorf tubes and centrifuged within 30 min of collection to separate plasma, and this fraction was frozen at −80 °C until analysis. Since the vast majority of circulating serotonin is stored in platelets, and because concentrations of 'free' serotonin in plasma have been reported to be far lower than what is found in serum and whole blood[13,46], it is possible that some degree of contamination from platelets occurred in our plasma samples during the collection process. To determine serotonin levels in BAT tissue, approximately 30–60 mg of BAT was homogenized in 0.2 N perchloric acid to precipitate proteins. The sample was centrifuged at 10,000 × *g* for 5 min, and the supernatant was collected. This fraction was then neutralized using an equal volume of borate buffer. Any remaining precipitate was removed by a second 10,000 × *g* centrifugation for 5 min, and the sample was frozen at −80 °C until analysis. Serotonin was analyzed in plasma and tissue samples using an enzymatic immunoassay kit (Beckman Coulter, Mississauga, Canada).

In vivo glucose uptake and body composition

Experiments were conducted as recently described[47,48]. Briefly, [^{18}F]fluorodeoxyglucose (FDG) was synthesized at McMaster University by the nucleophilic substitution method using an FDG synthesizing instrument (GE Healthcare, Milwaukee, WI, USA) and a cyclotron (Siemans 20–30 gb). Small-animal positron emission tomography (PET, Philip Mosaic, Andover, MA) and micro-computed tomography (CT) (Gamma Medica-Ideas Xspect System, NorthRidge, CA) imaging were performed using an acquisition time of 15 min for PET, followed by CT for 5 min. Images were reconstructed using the 3D-RAMLA algorithm, with no attenuation correction and no correction for partial-volume effects of the tomograph. Quantification was performed by Region-of-interest (ROI) analysis using Amide Research Workplace software, and FDG-tissue uptake was calculated using the mean value of standard uptake values (SUV). WAT FDG uptake was determined using an ROI within a region of intra-abdominal adipose tissue. Analysis of total body fat composition was determined by using Amira software (Visage Imaging), and the mean value of voxels of segmented adipose was calculated and expressed relative to total body mass[47].

Cell culture

An immortalized brown adipocyte (BA) cell line originally derived from mouse fetal brown fat[17] was cultured and differentiated. This cell line was validated and regularly tested for mycoplasma contamination. Briefly, confluent cells were placed in induction media (0.5 mM IBMX; 0.25 mM indomethacin; 2 μg ml^{-1} dexamethasone; 1 nM T3, 20 nM insulin) for 2 d and subsequently maintained on differentiation media (1 nM T3, 20 nM insulin). All experiments were performed on cultures 6–8 d post-induction. Unless otherwise indicated, cells were rinsed with PBS and media was changed to HEPES-buffered Krebs Ringer buffer (HKRB) + 1% BSA. Where indicated, BAs were treated with serotonin or indicated precursors and metabolites for 30 min (100 μM; Sigma) followed by isoproterenol (1 nM, Sigma) for 30 min or 4h, respectively, for western blotting or gene expression experiments. Stromal vascular cells (SVCs) from iWAT were differentiated with rosiglitazone (1 μM, Sigma) as previously described[49] and treated as above for BA except stimulation was performed with 10 nM isoproterenol.

Telemetric blood pressure and heart rate measurement

Male C57BL/6 mice (Jackson Labs) receiving HFD were anesthetized with isoflurane (4% induction, 1.5% maintenance) and were kept warm using an isothermal heat pad under aseptic conditions. Immediately upon induction of anesthesia, 50 μg kg^{-1} glycopyrrolate was administered subcutaneously to prevent excess airway secretions as well as 20 mg kg^{-1} ampicillin and 2 mg kg^{-1} Metacam (analgesic) via intramuscular injection. With the animal in the supine position, a midline incision was made in the skin of the neck region, and the underlying glandular tissue was separated by blunt dissection to expose the muscles of the neck. The left carotid artery was carefully dissected free of surrounding tissues and three 5-0 silk sutures (Harvard Apparatus) were passed underneath the vessel. The rostral suture was tied occlusively, whereas the caudal suture was used for temporary retraction of the vessel. A small incision was made in the vessel and the radiotelemeter catheter (Model: TA11–PAC10, Data Sciences International, St.Paul Minnesota) was introduced and advanced such that the tip entered the aortic arch. The catheter was sutured in place and the telemeter body was tunneled to a subcutaneous pocket along the right flank. The neck incision was closed with discontinuous sutures (4-0 Vicryl, Johnson & Johnson) and the animals recovered on a warming pad. 8–10 days were allowed for complete postoperative recovery before baseline 24-h telemetric recording of mean arterial pressure and heart rate. During all recordings, the animals were unrestrained in the home cage, with *ad libitum* access to food and water at all times. The home cage was placed on a Physio-Tel radiotelemeter receiver (Model: RPC-1, Data Sciences International), and data were recorded online via DataQuest ART Software (Data Sciences International). Following baseline recording, animals received one daily injection of either vehicle or the Tph1 inhibitor LP533401, prepared as described above. Recordings continued for 14 d of treatment, followed by a 3-d recovery period.

Analytical methods

For mRNA analysis, tissues were lysed in TRIzol reagent (Invitrogen, Carlsbad, CA, USA) and RNA extracted for qRT-PCR as described[47]. Immunoblotting of tissues was performed using antibodies from Cell Signaling (phospho–Akt^{S473}: #4058, total Akt: #9272, GAPDH:

#2118, phospho–HSL^{S660}: #4126, total HSL: #4107, phospho-PKA substrate: #9624), Invitrogen (β-tubulin: #322600) and Abcam (UCP1: #ab10983) as described[47] at a 1:1,000 dilution. For immunohistochemistry, paraffin-embedded eWAT, iBAT, and liver were sectioned, dewaxed and rehydrated before antigen retrieval as described[47]. The researcher examining the histological sections was blinded to the treatments. Liver and iBAT lipids were quantified in H&E-stained sections by segmenting out areas of the tissue that remained unstained using ImageJ. Obvious holes, edges and blood vessels were avoided. This quantification assumes that small round droplets are cellular lipids that remain unstained. cAMP levels were measured in brown adipocytes stimulated for 10 min with isoproterenol (1 nM). Cells or tissues were lysed with 0.1 M HCl, 0.2% Triton-X-100 for 20 min and neutralized with NaOH followed by centrifugation at 5,000 × *g* for 5 min and collection of the supernatant. cAMP levels were quantified in supernatants by ELISA (Biomedical Technologies Inc.). cAMP levels in iBAT were extracted and quantified by ELISA as suggested by the manufacturer (Cayman Chemical). Serum cytokines (IL-6 and Tnf-α) were measured via ELISA (R and D systems) on undiluted sample.

Statistical analysis

All data were found to be normally distributed. Results were analyzed using Student's *t*-test or ANOVA where appropriate, using GraphPad Prism software. When variances between groups were found to be different, a Welch's *t*-test was used. A repeated-measures ANOVA was used for all body weight plots, fed blood glucose and GTT and ITT data. A Bonferroni *post hoc* test was used to test for significant differences revealed by the ANOVA. Significance was accepted at $P \leq 0.05$. For animal experiments we have used a minimum of $n = 4$ for most measures as this gives us a power of 0.86 to detect significant differences in insulin sensitivity, our variable with the greatest variance.

Supplementary Material

Refer to Web version on PubMed Central for supplementary material.

Acknowledgments

These studies were supported by grants from the Canadian Diabetes Association (CDA) (J.R.B.D., G.R.S.) the Canadian Institutes of Health Research (CIHR) (J.R.B.D., W.I.K., G.R.S.), Crohn's and Colitis Canada (W.I.K.), the Natural Sciences and Engineering Research Council of Canada (G.R.S.) and the Faculty of Health Sciences at McMaster University to the MAC-Obesity Research Program (G.R.S., K.M.M.). E.P.M. is a CDA Postdoctoral Fellow, M.D.F. is a CIHR Banting Postdoctoral Fellow, A.C. was a Canadian Liver Foundation Summer Student, S.M.H. is a Heart & Stroke Foundation of Canada and Alberta Innovates Health Solutions Postdoctoral Fellow, J.D.S. is a CDA Scholar and W.I.K. is a CIHR New Investigator. G.R.S. is a Canada Research Chair in Metabolism and Obesity and the J. Bruce Duncan Chair in Metabolic Diseases.

References

1. Qiu Y, et al. Eosinophils and type 2 cytokine signaling in macrophages orchestrate development of functional beige fat. Cell. 2014; 157:1292–1308. [PubMed: 24906148]
2. Shabalina IG, et al. UCP1 in brite/beige adipose tissue mitochondria is functionally thermogenic. Cell Reports. 2013; 5:1196–1203. [PubMed: 24290753]
3. Cypess AM, et al. Identification and importance of brown adipose tissue in adult humans. N Engl J Med. 2009; 360:1509–1517. [PubMed: 19357406]

4. Ouellet V, et al. Outdoor temperature, age, sex, body mass index, and diabetic status determine the prevalence, mass, and glucose-uptake activity of ^{18}F-FDG-detected BAT in humans. J Clin Endocrinol Metab. 2011; 96:192–199. [PubMed: 20943785]
5. Saito M, et al. High incidence of metabolically active brown adipose tissue in healthy adult humans: effects of cold exposure and adiposity. Diabetes. 2009; 58:1526–1531. [PubMed: 19401428]
6. Berger M, Gray JA, Roth BL. The expanded biology of serotonin. Annu Rev Med. 2009; 60:355–366. [PubMed: 19630576]
7. Khan WI, Ghia JE. Gut hormones: emerging role in immune activation and inflammation. Clin Exp Immunol. 2010; 161:19–27. [PubMed: 20408856]
8. Walther DJ, et al. Synthesis of serotonin by a second tryptophan hydroxylase isoform. Science. 2003; 299:76. [PubMed: 12511643]
9. Kim HJ, et al. Metabolomic analysis of livers and serum from high-fat diet induced obese mice. J Proteome Res. 2011; 10:722–731. [PubMed: 21047143]
10. Kwak SH, et al. Association of variations in TPH1 and HTR2B with gestational weight gain and measures of obesity. Obesity (Silver Spring). 2012; 20:233–238. [PubMed: 21836641]
11. Tecott LH. Serotonin and the orchestration of energy balance. Cell Metab. 2007; 6:352–361. [PubMed: 17983581]
12. Alenina N, et al. Growth retardation and altered autonomic control in mice lacking brain serotonin. Proc Natl Acad Sci USA. 2009; 106:10332–10337. [PubMed: 19520831]
13. Sumara G, Sumara O, Kim JK, Karsenty G. Gut-derived serotonin is a multifunctional determinant to fasting adaptation. Cell Metab. 2012; 16:588–600. [PubMed: 23085101]
14. Ghia JE, et al. Serotonin has a key role in pathogenesis of experimental colitis. Gastroenterology. 2009; 137:1649–1660. [PubMed: 19706294]
15. Paulmann N, et al. Intracellular serotonin modulates insulin secretion from pancreatic beta-cells by protein serotonylation. PLoS Biol. 2009; 7:e1000229. [PubMed: 19859528]
16. Li Z, et al. Essential roles of enteric neuronal serotonin in gastrointestinal motility and the development/survival of enteric dopaminergic neurons. J Neurosci. 2011; 31:8998–9009. [PubMed: 21677183]
17. Uldry M, et al. Complementary action of the PGC-1 coactivators in mitochondrial biogenesis and brown fat differentiation. Cell Metab. 2006; 3:333–341. [PubMed: 16679291]
18. Liu Q, et al. Discovery and characterization of novel tryptophan hydroxylase inhibitors that selectively inhibit serotonin synthesis in the gastrointestinal tract. J Pharmacol Exp Ther. 2008; 325:47–55. [PubMed: 18192499]
19. Yadav VK, et al. Pharmacological inhibition of gut-derived serotonin synthesis is a potential bone anabolic treatment for osteoporosis. Nat Med. 2010; 16:308–312. [PubMed: 20139991]
20. Cohen P, et al. Ablation of PRDM16 and beige adipose causes metabolic dysfunction and a subcutaneous to visceral fat switch. Cell. 2014; 156:304–316. [PubMed: 24439384]
21. Schulz TJ, et al. Brown-fat paucity due to impaired BMP signalling induces compensatory browning of white fat. Nature. 2013; 495:379–383. [PubMed: 23485971]
22. Feldmann HM, Golozoubova V, Cannon B, Nedergaard J. UCP1 ablation induces obesity and abolishes diet-induced thermogenesis in mice exempt from thermal stress by living at thermoneutrality. Cell Metab. 2009; 9:203–209. [PubMed: 19187776]
23. Rapport MM, Green AA, Page IH. Serum vasoconstrictor, serotonin; isolation and characterization. J Biol Chem. 1948; 176:1243–1251. [PubMed: 18100415]
24. Hodges MR, et al. Defects in breathing and thermoregulation in mice with near-complete absence of central serotonin neurons. J Neurosci. 2008; 28:2495–2505. [PubMed: 18322094]
25. Breum L, Rasmussen MH, Hilsted J, Fernstrom JD. Twenty-four-hour plasma tryptophan concentrations and ratios are below normal in obese subjects and are not normalized by substantial weight reduction. Am J Clin Nutr. 2003; 77:1112–1118. [PubMed: 12716660]
26. Bertrand RL, et al. A Western diet increases serotonin availability in rat small intestine. Endocrinology. 2011; 152:36–47. [PubMed: 21068163]
27. Sullo A, Brizzi G, Maffulli N. Chronic peripheral administration of serotonin inhibits thyroid function in the rat. Muscles Ligaments Tendons J. 2011; 1:48–50. [PubMed: 23738246]

28. Srinivasan S, et al. Serotonin regulates *C. elegans* fat and feeding through independent molecular mechanisms. Cell Metab. 2008; 7:533–544. [PubMed: 18522834]
29. Ducy P, Karsenty G. The two faces of serotonin in bone biology. J Cell Biol. 2010; 191:7–13. [PubMed: 20921133]
30. Watts SW, Morrison SF, Davis RP, Barman SM. Serotonin and blood pressure regulation. Pharmacol Rev. 2012; 64:359–388. [PubMed: 22407614]
31. Gustafsson BI, et al. Long-term serotonin administration induces heart valve disease in rats. Circulation. 2005; 111:1517–1522. [PubMed: 15781732]
32. Stunes AK, et al. Adipocytes express a functional system for serotonin synthesis, reuptake and receptor activation. Diabetes Obes Metab. 2011; 13:551–558. [PubMed: 21320265]
33. Asghari R, Lung MSY, Pilowsky PM, Connor M. Sex differences in the expression of serotonin-synthesizing enzymes in mouse trigeminal ganglia. Neuroscience. 2011; 199:429–437. [PubMed: 22056601]
34. Kinoshita M, et al. Regulation of adipocyte differentiation by activation of serotonin (5-HT) receptors 5–HT2AR and 5–HT2CR and involvement of microRNA-448-mediated repression of KLF5. Mol Endocrinol. 2010; 24:1978–1987. [PubMed: 20719859]
35. Timmons JA, et al. Myogenic gene expression signature establishes that brown and white adipocytes originate from distinct cell lineages. Proc Natl Acad Sci USA. 2007; 104:4401–4406. [PubMed: 17360536]
36. Nichols DE, Nichols CD. Serotonin receptors. Chem Rev. 2008; 108:1614–1641. [PubMed: 18476671]
37. Izikki M, et al. Tryptophan hydroxylase 1 knockout and tryptophan hydroxylase 2 polymorphism: effects on hypoxic pulmonary hypertension in mice. Am J Physiol Lung Cell Mol Physiol. 2007; 293:L1045–L1052. [PubMed: 17675372]
38. Serra F, LeFeuvre RA, Slater D, Palou A, Rothwell NJ. Thermogenic actions of tryptophan in the rat are mediated independently of 5-HT. Brain Res. 1992; 578:327–334. [PubMed: 1511284]
39. Kiefer FW, et al. Retinaldehyde dehydrogenase 1 regulates a thermogenic program in white adipose tissue. Nat Med. 2012; 18:918–925. [PubMed: 22561685]
40. Roberts LD, et al. β-Aminoisobutyric acid induces browning of white fat and hepatic β-oxidation and is inversely correlated with cardiometabolic risk factors. Cell Metab. 2014; 19:96–108. [PubMed: 24411942]
41. Côté F, et al. Disruption of the nonneuronal *tph1* gene demonstrates the importance of peripheral serotonin in cardiac function. Proc Natl Acad Sci USA. 2003; 100:13525–13530. [PubMed: 14597720]
42. O'Neill HM, et al. AMP-activated protein kinase (AMPK) β1β2 muscle null mice reveal an essential role for AMPK in maintaining mitochondrial content and glucose uptake during exercise. Proc Natl Acad Sci USA. 2011; 108:16092–16097. [PubMed: 21896769]
43. Crane JD, Mottillo EP, Farncombe TH, Morrison KM, Steinberg GR. A standardized infrared imaging technique that specifically detects UCP1-mediated thermogenesis *in vivo*. Mol Metab. 2014; 3:490–494. [PubMed: 24944909]
44. Steinberg GR, et al. Whole body deletion of AMP-activated protein kinase β2 reduces muscle AMPK activity and exercise capacity. J Biol Chem. 2010; 285:37198–37209. [PubMed: 20855892]
45. Watt MJ, et al. CNTF reverses obesity-induced insulin resistance by activating skeletal muscle AMPK. Nat Med. 2006; 12:541–548. [PubMed: 16604088]
46. Cui Y, et al. Lrp5 functions in bone to regulate bone mass. Nat Med. 2011; 17:684–691. [PubMed: 21602802]
47. Galic S, et al. Hematopoietic AMPK β1 reduces mouse adipose tissue macrophage inflammation and insulin resistance in obesity. J Clin Invest. 2011; 121:4903–4915. [PubMed: 22080866]
48. Jorgensen SB, et al. Deletion of skeletal muscle SOCS3 prevents insulin resistance in obesity. Diabetes. 2013; 62:56–64. [PubMed: 22961088]
49. Ohno H, Shinoda K, Spiegelman BM, Kajimura S. PPARγ agonists induce a white-to-brown fat conversion through stabilization of PRDM16 protein. Cell Metab. 2012; 15:395–404. [PubMed: 22405074]

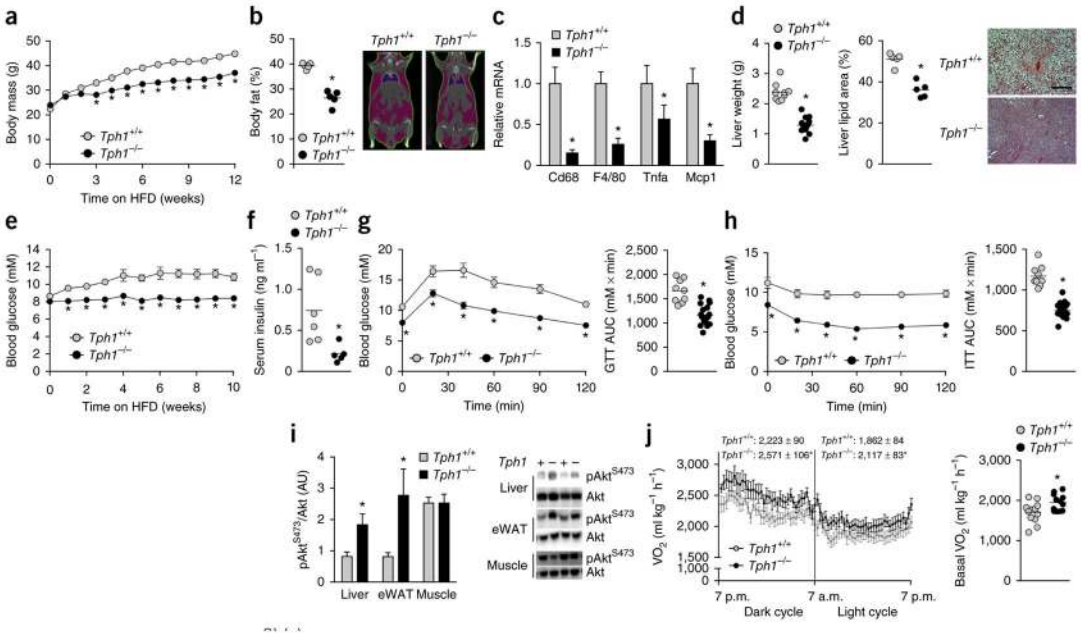

Figure 1.

Tph1$^{-/-}$ mice are protected from obesity, chronic low-grade inflammation, NALFD and insulin resistance. (**a**,**b**) Body mass ($n = 9$ *Tph1*$^{+/+}$ and $n = 19$ *Tph1*$^{-/-}$) (**a**) and adiposity (**b**) of HFD–fed *Tph1*$^{+/+}$ and *Tph1*$^{-/-}$ mice ($n = 5$ per group). Right (**b**), representative CT image. (**c**,**d**) eWAT inflammatory mRNA ($n = 8$) (**c**), liver weights ($n = 9$ *Tph1*$^{+/+}$ and $n = 19$ *Tph1*$^{-/-}$) and liver lipid area of HFD-fed *Tph1*$^{+/+}$ and *Tph1*$^{-/-}$ mice ($n = 5$ each group) (**d**). Right (**d**), representative liver cross-sections stained with H&E; scale bar is 100 μm. (**e**–**h**) Fed blood glucose over the course of the diet intervention ($n = 9$ *Tph1*$^{+/+}$ and $n = 19$ *Tph1*$^{-/-}$) (**e**), fasting serum insulin concentrations ($n = 6$ *Tph1*$^{+/+}$ and $n = 5$ *Tph1*$^{-/-}$) (**f**) and glucose tolerance test (GTT) (**g**) and insulin tolerance test (ITT) (**h**) performed after 10–12 weeks of HFD in *Tph1*$^{+/+}$ and *Tph1*$^{-/-}$ mice ($n = 9$ *Tph1*$^{+/+}$ and $n = 19$ *Tph1*$^{-/-}$). AUC area under the curve. (**i**) Akt^{S473} phosphorylation relative to total Akt in liver, eWAT and mixed gastrocnemius muscle from *Tph1*$^{+/+}$ and *Tph1*$^{-/-}$ mice killed 15 min following an injection of 0.5 U kg^{-1} insulin ($n = 4$ per group). AU, arbitrary units. (**j**) Oxygen consumption (VO_2) during light and dark cycles (left) and in the absence of movement (right) in HFD-fed *Tph1*$^{+/+}$ and *Tph1*$^{-/-}$ mice ($n = 12$ per group). Data are expressed as means ± s.e.m. *$P <$ 0.05 relative to *Tph1*$^{+/+}$ mice as determined using a Student's *t*-test or two-way repeated measures analysis of variance (ANOVA) and Bonferroni *post hoc* test.

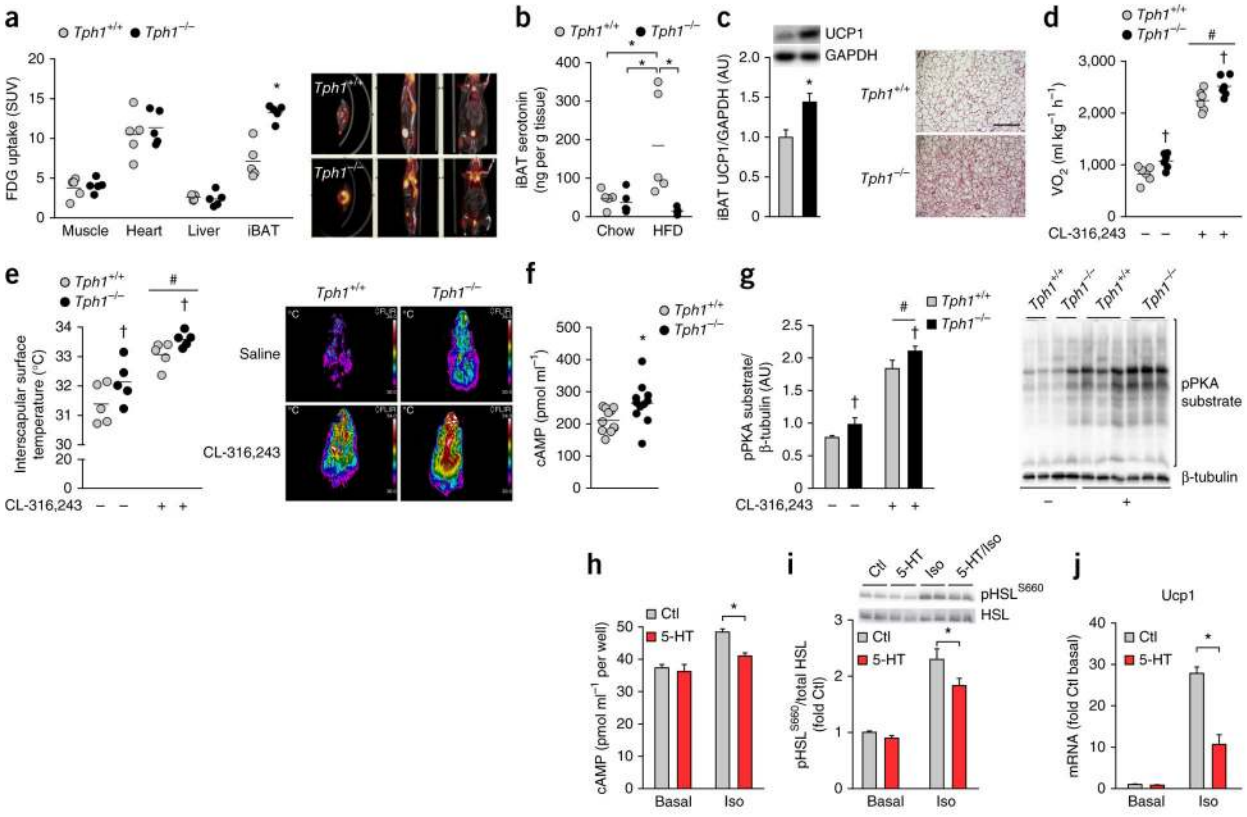

Figure 2.

Mice lacking Tph1 have increased metabolic rate and brown adipose tissue activity due to an inhibition of β–adrenergic signaling by serotonin. (**a**) Tissue FDG uptake in *Tph1*$^{+/+}$ and *Tph1*$^{-/-}$ mice fed a HFD ($n = 5$ per group). SUV, standardized uptake values. (**b**,**c**) iBAT serotonin content determined by ELISA ($n = 5$ per group) (**b**) and UCP1 protein content ($n = 8$ *Tph1*$^{+/+}$ and $n = 7$ *Tph1*$^{-/-}$) (left, **c**) from iBAT of *Tph1*$^{+/+}$ and *Tph1*$^{-/-}$ mice fed a HFD as assessed by western blot (top, **c**) and tissue sections stained with H&E (right, **c**; scale bar is 50 μm). AU, arbitrary units. (**d**,**e**) Oxygen consumption ($n = 6$ per group) (**d**) and dorsal interscapular surface temperature (**e**) of anesthetized HFD-fed *Tph1*$^{+/+}$ and *Tph1*$^{-/-}$ mice following injection with saline or CL-316,243 ($n = 5$ per group). Right (**e**), representative thermal images of mice injected with saline or CL-316,243. (**f**) cAMP levels determined by ELISA in iBAT of HFD–fed *Tph1*$^{+/+}$ and *Tph1*$^{-/-}$ mice ($n = 11$ per group). (**g**) Relative PKA substrate phosphorylation in iBAT of HFD-fed *Tph1*$^{+/+}$ and *Tph1*$^{-/-}$ mice 15 min following an injection of saline or CL-316,243 ($n = 5$ per group, right: representative western blot). (**h**–**j**) cAMP ($n = 3$ per treatment in two separate experiments) (**h**) HSL phosphorylation (S660, $n = 5$ per treatment in two separate experiments) (**i**) and Ucp1 mRNA (**j**) in control and isoproterenol-stimulated brown adipocytes ($n = 4$ per treatment in two separate experiments). Data are expressed as means ± s.e.m. $^{*}P < 0.05$ relative to *Tph1*$^{+/+}$ mice or Ctl, $^{\#}P < 0.05$ relative to saline or $^{\dagger}P < 0.05$ versus *Tph1*$^{+/+}$ as determined using a Student's *t*-test or, where appropriate, a two-way analysis of variance (ANOVA) and Bonferroni *post hoc* test.

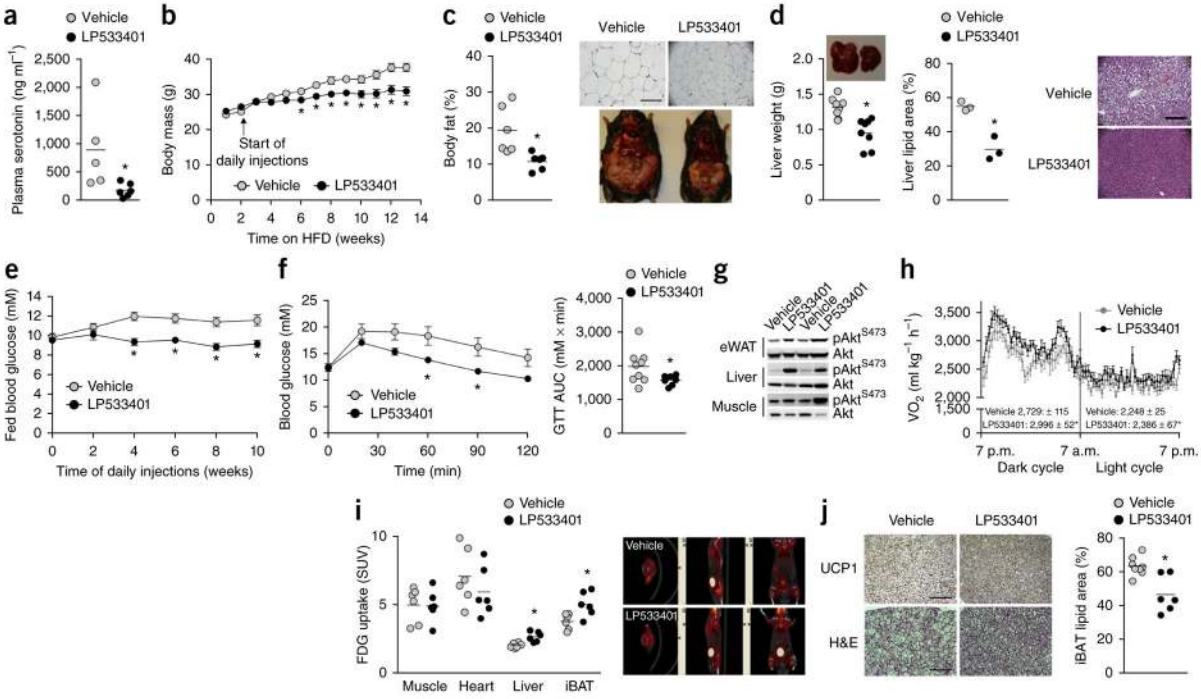

Figure 3.

Chemical inhibition of Tph1 prevents obesity and insulin resistance and increases brown adipose tissue activity and UCP1 expression in HFD-fed C57BL/6 mice. (**a**) Plasma serotonin concentrations of HFD-fed C57BL/6 mice after 8 weeks of LP533401 treatment (n = 5 vehicle and n = 6 LP533401 treated). (**b**) Body mass of HFD-fed C57BL/6 mice over 14 weeks treated with vehicle or LP533401 for the last 12 weeks (n = 9 vehicle and n = 8 LP533401). (**c**) Adiposity of vehicle- and LP533401-treated mice (n = 6 vehicle and LP533401). Top right, H&E-stained sections of eWAT, scale bar is 100 μm; bottom right, representative images of mice from each treatment group. (**d**) Liver weight (n = 9 vehicle and n = 8 LP533401) and lipid area fraction (n = 3 vehicle and LP533401) in vehicle- and LP533401-treated, HFD-fed mice. Right, H&E-stained sections of liver from vehicle- and LP533401-treated, HFD-fed mice; scale bar is 100 μm. (**e**,**f**) Fed blood glucose over the treatment period (**e**) and GTT (**f**) of vehicle- and LP533401-treated, HFD-fed mice and AUC. n = 9 vehicle and n = 8 LP533401 for all three graphs. (**g**) Akt^{S473} phosphorylation relative to total Akt in liver, eWAT and mixed gastrocnemius muscle from vehicle- and LP533401-treated mice 15 min following an injection of 0.5 U kg^{-1} insulin (n = 9 vehicle and n = 8 LP533401). (**h**,**i**) Oxygen consumption during light and dark cycles (n = 7 per group) (**h**) and tissue FDG uptake (n = 6 per group) (**i**) in vehicle- and LP533401-treated mice. Right (**i**), representative PET-CT images from each group. (**j**) Representative immunohistochemical staining of UCP1 (top, scale bar is 100 μm) and H&E (bottom, scale bar is 50 μm) representative of 8 vehicle- and 6 LP533401-treated mice and lipid area fraction in iBAT (right) from mice treated with vehicle or LP533401 (n = 8 vehicle and n = 6 LP533401). Data are expressed as means ± s.e.m. *P < 0.05 compared to vehicle as determined using a Student's t-test or, where appropriate, using a two-way repeated measures ANOVA.

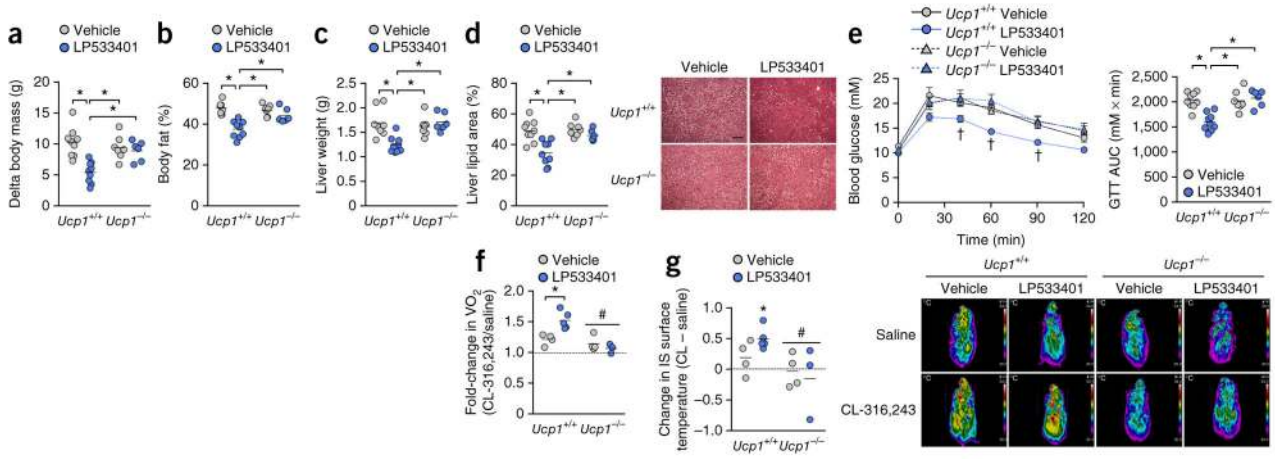

Figure 4.

UCP1 expression is required for the metabolic benefits of Tph1 inhibition. (**a**,**b**) Change in body mass after 6 weeks of HFD (**a**) and adiposity (**b**) from vehicle- and LP533401- treated *Ucp1*$^{+/+}$ and *Ucp1*$^{-/-}$ mice. (**c**,**d**) Liver mass (**c**) and lipid content (**d**; right, representative H&E cross-sections) in vehicle- and LP533401- treated mice. Scale bar is 100 μm. (**e**) GTT and AUC of vehicle- and LP533401-treated *Ucp1*$^{+/+}$ and *Ucp1*$^{-/-}$ mice. For **a**–**e**, $n = 9$ for *Ucp1*$^{+/+}$ vehicle and LP533401, $n = 7$ for *Ucp1*$^{-/-}$ vehicle and $n = 6$ for *Ucp1*$^{-/-}$ LP533401. (**f**,**g**) Change in oxygen uptake (**f**) and dorsal interscapular surface temperature (**g**) in vehicle- and LP533401-treated mice acutely injected with saline or CL-316,243 ($n = 4$ for *Ucp1*$^{+/+}$ and *Ucp1*$^{-/-}$ vehicle, $n = 5$ for *Ucp1*$^{+/+}$ LP533401 and $n = 3$ for *Ucp1*$^{-/-}$ LP533401). Right (**g**), representative thermal images of all mice in a given group. Data are expressed as means ± s.e.m. $^{*}P < 0.05$ relative to indicated groups or versus saline condition. $^{\#}P < 0.05$ relative to wild-type and $^{\dagger}P < 0.05$ relative to all other groups as determined by two-way ANOVA and Bonferroni *post hoc* test.